

Supplemental Material for “Long-Range Correlations in Elastic Moduli and Local Stresses at the Unjamming Transition”

Surajit Chakraborty* and Kabir Ramola†
Tata Institute of Fundamental Research, Hyderabad 500046, India

In this Supplemental Material, we provide additional details related to the results presented in the main text. We provide measures of the bulk modulus correlations in Fourier space at different pressures. We analyze the behavior of the elasticity lengthscale at the approach to unjamming. We provide measures of the correlations of the shear modulus in real space. Finally, we analyze the behavior of the unjamming transition for systems with different repulsive interactions.

I. BULK MODULUS CORRELATION

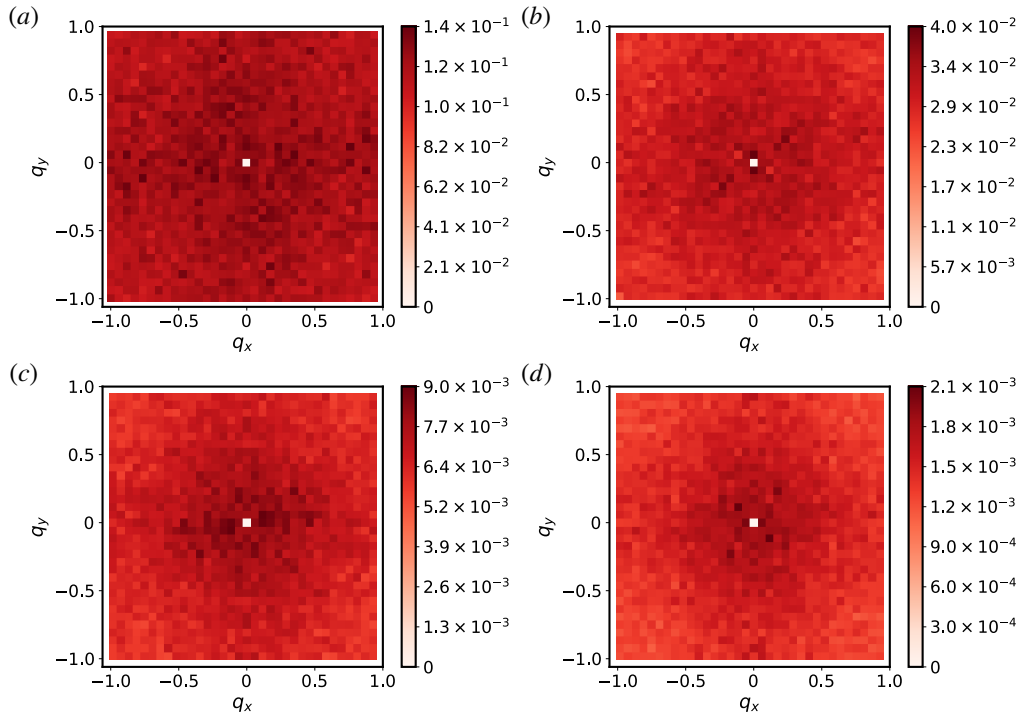


FIG. 1. Bulk modulus correlations in Fourier space for two-dimensional amorphous packings of $N = 8192$ disks with Hertzian repulsion at various pressures: (a) $p = 10^{-3}$, (b) $p = 10^{-4}$, (c) $p = 10^{-5}$, and (d) $p = 10^{-6}$. The correlations are independent of \vec{q} , indicating negligible correlation at large distances. The local bulk modulus in real space is measured using coarse-grained boxes of size $l_w = 3$.

In this section, we illustrate the bulk modulus correlation measured in Fourier space. The bulk modulus is primarily dominated by its affine component, with the non-affine contribution being relatively small. We perform a discrete Fourier transform of ΔK_m^A , representing the difference between K_m^A and its spatially averaged value \bar{K}_m^A ,

$$\Delta K_m^A(\vec{q}) = \sum_m \exp(i\vec{q} \cdot \vec{r}_m) \Delta K_m^A. \quad (1)$$

* schakraborty@tifrh.res.in

† kramola@tifrh.res.in

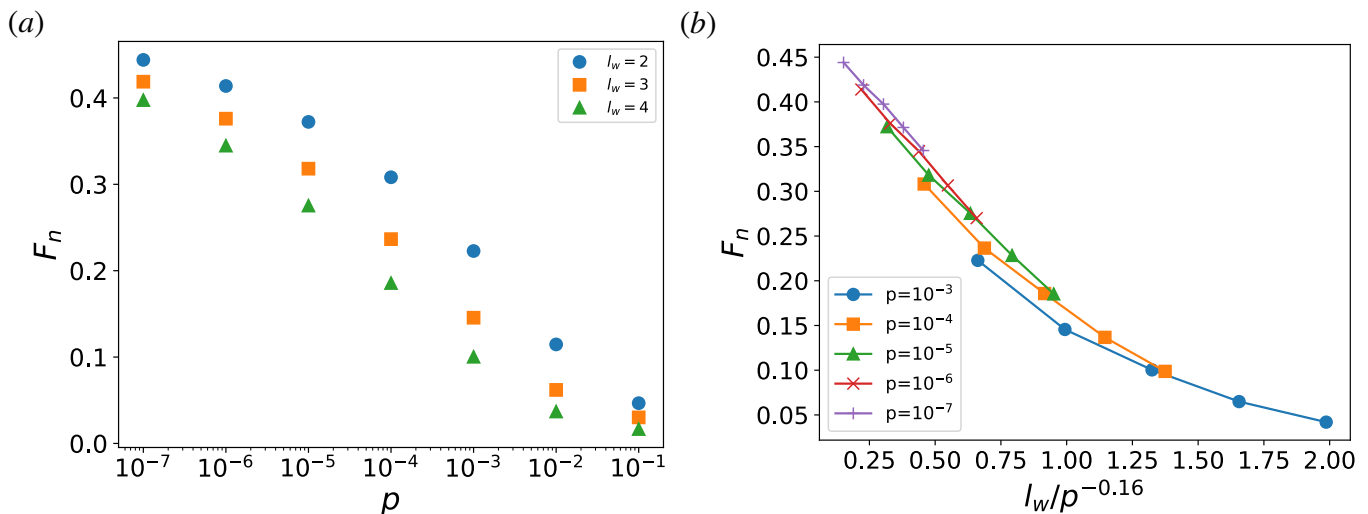


FIG. 2. (a) Fraction of negative shear modulus region as a function of pressure. (b) Scaling collapse of $F_n(l_w, p)$ reveals a length scale that diverges as $p^{-0.16}$ as the system approaches unjamming.

The correlation in Fourier space is given by,

$$C_G^A(\vec{q}) = \langle \Delta G_m^A(\vec{q}) \Delta G_m^A(-\vec{q}) \rangle. \quad (2)$$

Fig. 1 illustrates the Fourier space representation of bulk modulus correlation across different pressures. In Fourier space, the correlations appear independent of \vec{q} , displaying isotropic and radially independent behavior near $|q| \rightarrow 0$. This implies a negligible correlation in local bulk modulus across significant spatial distances, similar to pressure correlations observed in amorphous solids [1].

II. ELASTICITY LENGTHSCALE OF JAMMED SOLIDS

The presence of quasi-localized excitations leads to non-affine relaxation of particles when deformed in mechanical equilibrium. At small length scales, the non-affine response becomes substantial, resulting in regions with a negative modulus.

In Fig. 2 (a), we measure the fraction of regions with a negative shear modulus, defined as:

$$F_n = \int_{G_m < 0} P(G_m), dG_m. \quad (3)$$

As the unjamming transition is approached ($p \rightarrow 0$), F_n increases, indicating a large number of unstable regions as the system becomes more fragile. The number of unstable regions decreases when measured using larger coarse-grained boxes, suggesting the existence of a length scale above which elasticity is recovered. A crossover length scale can be constructed beyond which this phenomenon occurs. From the scaling collapse of $F_n(p, l_w)$ shown in Fig. 2 (b), we identify a length scale that diverges as $p^{-0.16}$ as the system approaches $p \rightarrow 0$, consistent with the isostatic length scale scaling in two dimensions [2]. Mizuno *et al.* [3] have reported the same scaling behavior for the length scale at which the relative fluctuations become negligible.

III. SHEAR MODULUS CORRELATION IN REAL SPACE

In this section, we present the shear modulus correlation in real space, $\langle \Delta G(\vec{r}) \Delta G(0) \rangle$. The shear modulus correlation exhibits long-range correlations with a quadrupole shape. This large-scale behavior is evident from the presence of non-vanishing anisotropic correlations as $|q| \rightarrow 0$. Fig. 3 illustrates the real space correlations across different pressures for packings of $N = 8192$ disks interacting via Hertzian interactions.

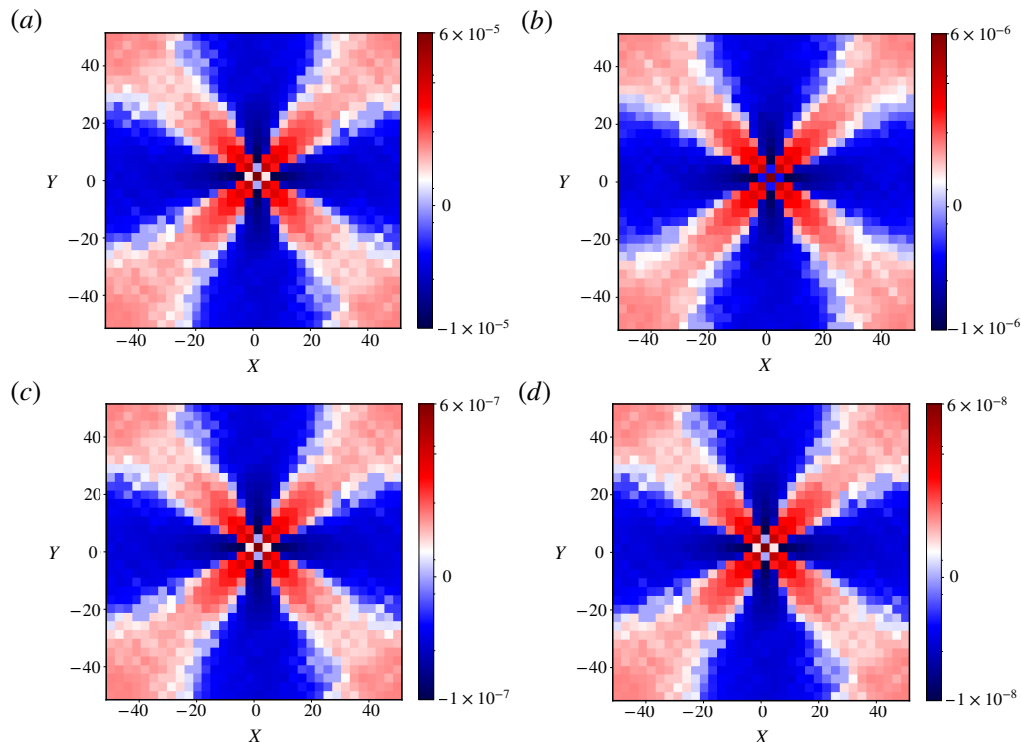


FIG. 3. The shear modulus correlation in real space for a packing of $N = 8192$ disks with Hertzian repulsion at different pressures: **(a)** $p = 10^{-3}$, **(b)** $p = 10^{-4}$, **(c)** $p = 10^{-5}$, and **(d)** $p = 10^{-6}$. The local moduli are measured using coarse-grained boxes with a linear width of $l_w = 3$. The local shear moduli exhibit long-range anisotropic correlations, manifesting a quadrupole shape at all pressures up to the unjamming point.

TABLE I. Scaling behavior of mean bulk modulus (\bar{K}_m), mean shear modulus (\bar{G}_m), stress correlation strength (A), and shear modulus correlation strength (g) with pressure as the system approaches the unjamming transition across various repulsive strengths (α).

| α | \bar{K}_m | \bar{G}_m | A | g |
|----------|-------------|-------------|-------|------------|
| 2 | p^0 | $p^{0.5}$ | p^2 | $p^{0.5}$ |
| 2.5 | $p^{0.33}$ | $p^{0.66}$ | p^2 | p^1 |
| 3 | $p^{0.5}$ | $p^{0.75}$ | p^2 | $p^{1.25}$ |
| 3.5 | $p^{0.6}$ | $p^{0.8}$ | p^2 | $p^{1.30}$ |
| 4 | $p^{0.66}$ | $p^{0.83}$ | p^2 | $p^{1.40}$ |
| 4.5 | $p^{0.714}$ | $p^{0.857}$ | p^2 | $p^{1.45}$ |

IV. THE UNJAMMING TRANSITION BEHAVIOR ACROSS VARIOUS REPULSIVE STRENGTH

This section illustrates the unjamming transition behavior for various repulsive strengths (α). Fig. 4 presents the scaling behavior of different quantities as pressure approaches the unjamming point for distinct values of α . Panels **(a)** through **(d)** in the figure show the scaling behaviour at the unjamming point for: **(a)** mean bulk modulus (\bar{K}_m), **(b)** mean shear modulus (\bar{G}_m), **(c)** stress correlation amplitude (A), and **(d)** shear modulus correlation amplitude (g). The scaling exponents associated with these quantities are listed in TABLE I.

For all α values, the mean bulk modulus scales as $p^{(\alpha-2)/(\alpha-1)}$, while the mean shear modulus follows a scaling of $p^{(\alpha-\frac{3}{2})/(\alpha-1)}$, as shown in Fig. 4 **(a)** and **(b)**, respectively. These power-law behaviors in the mean moduli are similar to those observed in the jamming of soft repulsive spheres [4–6].

Stress correlations behave as $C_{xyxy}(q, \theta) = A \sin^2 \theta \cos^2 \theta$ as $|q| \rightarrow 0$, with A varying with the pressure (p) of the packings. Notably, stress correlations in jammed solids exhibit a universal characteristic, showing a quadratic decay of A , i.e. $A \sim p^2$ as pressure approaches the unjamming point, independent of specific interaction details, as shown in Fig. 4 **(c)**. Shear modulus correlation exhibits a similar structural pattern to shear stress correlation,

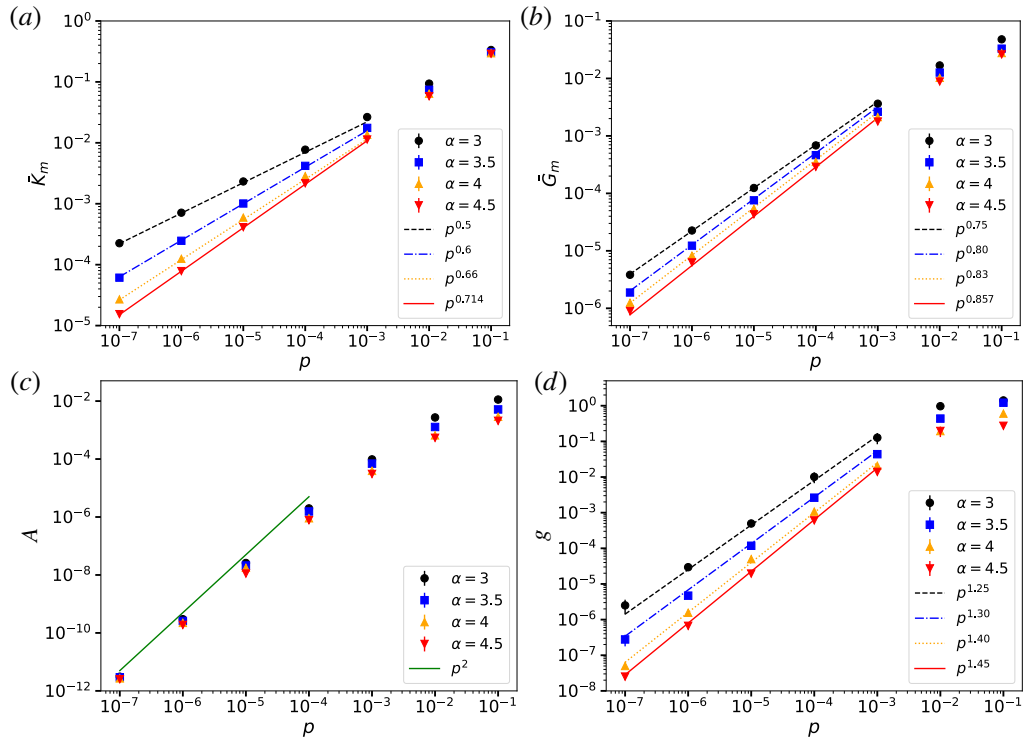


FIG. 4. Dependence of various characteristics on the pressure of the solids is illustrated for different values of α : (a) mean bulk modulus (\bar{K}_m), (b) mean shear modulus (\bar{G}_m), (c) stress correlation strength (A), and (d) shear modulus correlation strength (g).

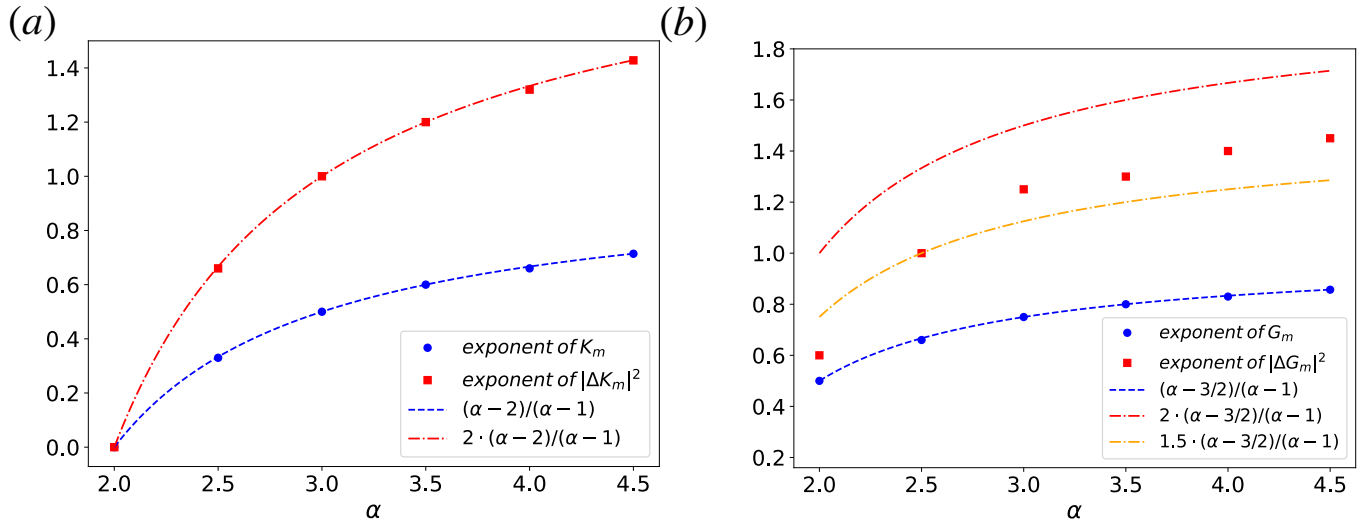


FIG. 5. (a) Bulk modulus fluctuations exhibit a scaling behavior of $p^{2(\alpha-2)/(\alpha-1)}$, while the mean bulk modulus scales as $p^{(\alpha-2)/(\alpha-1)}$. (b) In contrast, shear modulus fluctuations display anomalous behavior, lacking consistent correlation strength behavior with α . However, the mean shear modulus scales as $p^{(\alpha-\frac{3}{2})/(\alpha-1)}$.

$C_G(q, \theta) = g \sin^2 \theta \cos^2 \theta$ as $|q| \rightarrow 0$, with g varying with the pressure (p) of the packings. However, the behavior of modulus correlations depends on the model, with g decaying according to power-law exponents that vary based on the specific interaction potential, as illustrated in Fig. 4 (d).

Fluctuations in the local bulk moduli scale with their spatial average; i.e. $|\Delta K_m|$ and \bar{K}_m both scale as $p^{(\alpha-2)/(\alpha-1)}$ as pressure decreases towards the unjamming point for different values of α , as shown in Fig. 5 (a). In contrast, the total shear modulus, which includes significant non-affine contributions, exhibits anomalous scaling behavior. Notably,

no consistent relation is observed between the shear modulus fluctuations and the exponent of the interaction potential, as shown in Fig. 5 (b). However, the mean shear modulus scales as $p^{(\alpha-\frac{3}{2})/(\alpha-1)}$ as the unjamming transition is approached for different values of α .

-
- [1] J. N. Nampoothiri, M. D'Eon, K. Ramola, B. Chakraborty, and S. Bhattacharjee, Tensor electromagnetism and emergent elasticity in jammed solids, *Physical Review E* **106**, 065004 (2022).
 - [2] E. Lerner, E. DeGiuli, G. Düring, and M. Wyart, Breakdown of continuum elasticity in amorphous solids, *Soft Matter* **10**, 5085 (2014).
 - [3] H. Mizuno, L. E. Silbert, and M. Sperl, Spatial distributions of local elastic moduli near the jamming transition, *Physical review letters* **116**, 068302 (2016).
 - [4] C. S. O'hern, L. E. Silbert, A. J. Liu, and S. R. Nagel, Jamming at zero temperature and zero applied stress: The epitome of disorder, *Physical Review E* **68**, 011306 (2003).
 - [5] W. G. Ellenbroek, E. Somfai, M. van Hecke, and W. van Saarloos, Critical scaling in linear response of frictionless granular packings near jamming, *Physical review letters* **97**, 258001 (2006).
 - [6] V. Vitelli, N. Xu, M. Wyart, A. J. Liu, and S. R. Nagel, Heat transport in model jammed solids, *Physical Review E* **81**, 021301 (2010).